



---

## **SUPPORT SERVICES FOR CERAMIC FIBER-CERAMIC MATRIX COMPOSITES**

Annual Technical Progress Report

September 20, 1995

Research sponsored by the U.S. Department of Energy,  
Fossil Energy  
Advanced Research and Technology Development Materials Program

Report Prepared by  
John P. Hurley  
Energy & Environmental Research Center  
University of North Dakota  
PO Box 9018  
Grand Forks, ND 58202-9018  
under  
19X-SS112V

for

OAK RIDGE NATIONAL LABORATORY  
Oak Ridge, Tennessee 37831  
managed by  
LOCKHEED MARTIN ENERGY SYSTEMS, INC.  
for the  
U.S. Department of Energy  
under Contract No. DE-AC05-84OR21400

**MASTER**

This report has been reproduced directly from the best available copy.

Available to DOE and DOE contractors from the Office of Scientific and Technical Information, PO Box 62, Oak Ridge, TN 37831; prices available from (615) 576-8401, FTS 626-8401.

Available to the public from the National Technical Information Service, U.S. Department of Commerce, 5285 Port Royal Road, Springfield, VA 22161.

This report was prepared as an account of work sponsored by an agency of the United States Government. Neither the United States Government nor any agency thereof, nor any of their employees, makes any warranty, expressed or implied, or assumes any legal liability or responsibility for the accuracy, completeness, or usefulness of any information, apparatus, product, or process disclosed, or represents that its use would not infringe privately owned rights. Reference herein to any specific commercial product, process, or service by trade name, trademark, manufacturer, or otherwise, does not necessarily constitute or imply its endorsement, recommendation, or favoring by the United States Government or any agency thereof. The views and opinions of authors expressed herein do not necessarily state or reflect those of the United States Government or any agency thereof.

## **DISCLAIMER**

**Portions of this document may be illegible  
in electronic image products. Images are  
produced from the best available original  
document.**

## TABLE OF CONTENTS

|                                                                                          |     |
|------------------------------------------------------------------------------------------|-----|
| LIST OF FIGURES .....                                                                    | ii  |
| LIST OF TABLES .....                                                                     | iii |
| 1.0 INTRODUCTION .....                                                                   | 1   |
| 2.0 FACTORS AFFECTING THE COMPOSITION OF ASH DEPOSITS .....                              | 1   |
| 2.1 Coal-Related Factors .....                                                           | 2   |
| 2.2 Factors Related to Ash Deposition Mechanisms .....                                   | 3   |
| 2.3 Factors Related to the Temperature of the Material .....                             | 5   |
| 3.0 THE EFFECTS OF SPECIFIC ELEMENTS IN THE CORROSION<br>OF SILICON-BASED CERAMICS ..... | 8   |
| 3.1 Combustion Conditions .....                                                          | 9   |
| 3.2 Gasification Conditions .....                                                        | 11  |
| 4.0 SUMMARY .....                                                                        | 12  |
| 5.0 REFERENCES .....                                                                     | 16  |

## LIST OF FIGURES

|   |                                                                                                                                                                                                                                                               |    |
|---|---------------------------------------------------------------------------------------------------------------------------------------------------------------------------------------------------------------------------------------------------------------|----|
| 1 | Comparison of the compositions (SO <sub>3</sub> -free) of the aerodynamically sized entrained ash particles and a conventional fouling deposit . . . . .                                                                                                      | 4  |
| 2 | Comparison of the compositions (SO <sub>3</sub> -free) of the aerodynamically sized entrained ash particles and an upstream enamel deposit . . . . .                                                                                                          | 4  |
| 3 | Temperature-dependent concentrations of silicon, sulfur, and calcium (reported as oxides) in deposits collected from the convective pass of a pulverized coal-fired utility boiler burning a subbituminous coal from the western United States . . . . .      | 5  |
| 4 | Temperature-dependent concentrations of sodium, potassium, and phosphorus (reported as oxides) in deposits collected from the convective pass of a pulverized coal-fired utility boiler burning a subbituminous coal from the western United States . . . . . | 6  |
| 5 | Viscosity-versus-temperature plot for a slag produced in a boiler firing Illinois No. 6 bituminous coal to which limestone has been added to reduce slag viscosity . . . . .                                                                                  | 7  |
| 6 | Scanning electron micrograph of a cross section of Hexoloy SA silicon carbide (bottom) exposed to Illinois No. 6 slag at (top) 2300°F in a static slag corrosion test in air . . . . .                                                                        | 7  |
| 7 | Scanning electron micrograph of the interface between siliconized silicon carbide (bottom) and a high-calcium ash doped with excess sodium sulfate (top) reacted at 1790°F . . . . .                                                                          | 8  |
| 8 | Viscosity-versus-temperature curves in air and reducing conditions for the three slags listed in Table 2. (a) Riverside Powder River Basin slag<br>(b) Baldwin Illinois No. 6 slag . . . . .                                                                  | 13 |

## LIST OF TABLES

|   |                                                                                     |    |
|---|-------------------------------------------------------------------------------------|----|
| 1 | Coal Ash Chemical Composition Ranges . . . . .                                      | 2  |
| 2 | Chemical Compositions of Standard Ashes . . . . .                                   | 12 |
| 3 | Typical Operating Conditions for the Main Types of Oxygen-Blown Gasifiers . . . . . | 14 |

## SUPPORT SERVICES FOR CERAMIC FIBER-CERAMIC MATRIX COMPOSITES

*Research sponsored by the U.S. Department of Energy, Fossil Energy Advanced Research and Technology Development Materials Program, DOE/FE AA 15 10 10 0, Work Breakdown Structure Element UNDEERC-4*

### 1.0 INTRODUCTION

To increase national self-sufficiency for the near future, energy systems will be required to fire low-grade fuels in a more efficient manner than currently possible. The coal-fired steam cycle used at present is limited to a maximum steam temperature of 550°C and a conversion efficiency of 35%. Higher working-fluid temperatures are required to boost efficiency exposing subsystems to much more corrosive environments. Issues of special concern to ceramists are corrosion and blinding of hot-gas particulate filters and catastrophic failure of high-temperature ceramic heat exchangers. To prevent those structures from failing will require a better understanding of the limits of their usability.

The University of North Dakota Energy & Environmental Research Center (EERC) is providing technical assistance and coal by-products to the Advanced Research and Technology Development (AR&TD) Materials Program investigating ceramic corrosion in fossil energy systems. The main activities for this year were to assemble coal slag and hot-gas filter ash samples for use by corrosion researchers and to initiate discussions within the ceramics and fossil energy communities on appropriate test conditions for materials to be used in fossil energy systems. Those activities are discussed in this report, which is an extension of a technical paper entitled "Factors Affecting the Corrosion Rates of Ceramics in Coal Combustion Systems," presented at the Ninth Annual Fossil Energy Materials Conference in Oak Ridge, Tennessee (1).

The corrosion discussion focuses primarily on silicon- and alumina-based ceramics because they are most often considered for the construction of large subsystems. However, only a few studies have been performed with the materials in actual coal combustion environments (2-6) and even fewer in gasification environments. Testing is especially difficult because of the complexity of coal-fueled energy systems and the great variability in coal ash compositions.

In this report, fuel and operational factors that affect the corrosion rates of structural ceramics in coal-fired combustor systems are described, with examples of the corrosion of silicon carbide-based materials. Particular attention is focused on two subsystems, hot-gas particulate filtration and high-temperature heat exchangers. Gasification systems are also discussed in an effort to acquaint the reader with the complexities of testing in gasification environments. The objective of the report is not to present specific data on rate factors, but to help the experimentalist measuring these factors to better design tests.

### 2.0 FACTORS AFFECTING THE COMPOSITION OF ASH DEPOSITS

All surfaces of a coal-fired combustor upstream of particulate removal systems are quickly covered with ash. The composition of the ash deposits depends on the composition of the coal, the mechanisms of ash deposition, and the temperature of the deposits.

## 2.1 Coal-Related Factors

Coal is composed primarily of carbon with lesser amounts of heteroatoms such as hydrogen, oxygen, sulfur, and nitrogen and ash-forming constituents such as mineral matter and organically associated alkali and alkaline-earth cations. The quantity and form of the major elements in the coal are determined by the original plants, the depositional environment, and the interaction of the buried material with groundwater before and after coalification.

Coals from the eastern United States are typically high-rank coals that form ash from microscopically observable mineral grains. The most prevalent minerals in U.S. coals are quartz ( $\text{SiO}_2$ ), kaolinite ( $\text{Al}_2\text{Si}_2\text{O}_5[\text{OH}]_4$ ), other aluminosilicate clays such as montmorillonite ( $[\text{Al},\text{Mg}]_8[\text{Si}_4\text{O}_{10}]_3[\text{OH}]_{10}\cdot 12\text{H}_2\text{O}$ ) and illite ( $\text{KAl}_5\text{Si}_7\text{O}_{20}[\text{OH}]_4$ ), and pyrite ( $\text{FeS}_2$ ). These minerals are rich in silicon, aluminum, and iron, so the coal ash is acidic. Coals from the western United States also contain these minerals, but they are primarily lower-rank coals that have undergone less lithification than the eastern coals and so contain much more oxygen in their organic structures. The oxygen is commonly present in carboxylic acid functional groups. During interaction with groundwater, these acids can undergo ion exchange to fix sodium, potassium, magnesium, and calcium in an atomically disbursed form within the organic structure. The addition of the alkali metal and alkaline-earth elements to the ash make it much more basic than eastern coal ash.

Because of the large range of depositional environments, degrees of coalification, and interactions with groundwater, U.S. coal ashes have a wide range of compositions. Table 1 shows the range as given in a standard text (7). This wide range of compositions requires the materials researcher to consider specific coals that may be used in the energy system of interest.

TABLE 1

| Coal Ash Chemical Composition Ranges |            |
|--------------------------------------|------------|
| Oxide Component                      | Percentage |
| $\text{SiO}_2$                       | 10–70      |
| $\text{Al}_2\text{O}_3$              | 8–38       |
| $\text{Fe}_2\text{O}_3$              | 2–50       |
| $\text{CaO}$                         | 0.5–30     |
| $\text{MgO}$                         | 0.3–8      |
| $\text{Na}_2\text{O}$                | 0.1–8      |
| $\text{K}_2\text{O}$                 | 0.1–3      |
| $\text{SO}_3$                        | 0.1–30     |

## 2.2 Factors Related to Ash Deposition Mechanisms

In addition to the type of coal that may be used in the energy system, the experimentalist must consider which fractions of the ash will come in contact with the ceramic. This information is best obtained experimentally, although approximations can be made based on extensive testing performed at utility boilers. During combustion of the coal, the minerals can vaporize, fragment, or coalesce, depending on the initial association of the mineral with the coal, the temperature and gas composition of the local combustion environment, and the morphology of the original mineral grains (8–13). In general, mineral grains that are included within coal particles will experience temperatures 200°–300°C higher and much more reducing conditions than the excluded mineral grains that are separate from the carbonaceous particles. The included minerals commonly fuse with other mineral grains in the particle to form larger, more compositionally complex ash particles. The excluded mineral grains are much less likely to interact with other mineral grains. A fraction may also fragment to form smaller ash particles.

In contrast to the mineral grains, the organically associated elements vaporize during combustion and become extremely reactive. The alkaline earth elements rapidly oxidize to form micron-sized ash particles on the surface of the burning char particle. These can be shed as oxide particles or coalesce with quartz- and clay-derived ash to form complex aluminosilicates (8, 9). In contrast, the vaporized alkali metals exist as gaseous sulfates, hydroxides, and chlorides that can condense far downstream of the fireball. The vaporization and subsequent condensation of the organically associated elements cause them to concentrate in smaller ash particles.

The size and composition interdependence in the ash means that the composition of the ash depositing on and possibly corroding the material of interest may be very different from the bulk ash because the size of ash that deposits depends on the local gas flow conditions. If the object of interest is a tube placed directly in the gas flow, then larger ash particles will separate from the gas flow and strike the tube as the gas diverges around it, while the smaller ash will stay entrained with the gas. Figure 1 illustrates the results of this separation. It compares the compositions of an ash deposit formed at 2100°F on the upstream side of a steam tube with four aerodynamic size ranges of particulate ash collected from the boiler at the same location (14). The boiler was firing a high-calcium subbituminous coal at the time. The most striking variations in elemental concentration versus ash particle size occur for silicon and calcium. The average concentration of silicon is much greater in the larger particles, whereas the average concentration of calcium is much greater in the smaller. This characteristic of the ash is typical of most high-calcium U.S. coals. The bulk composition of the deposit shows that it is formed primarily from particles with aerodynamic diameters of over 10  $\mu\text{m}$ .

Figure 2 shows the compositions of another type of ash deposit along with aerodynamically sized ash collected in the vicinity. This type of deposit also forms on the upstream sides of steam tubes when firing high-calcium coals but forms at temperatures below approximately 1700°F. A comparison of the compositions shows that these deposits form predominantly from particles with aerodynamic diameters below 3  $\mu\text{m}$  and so are greatly enriched in calcium and depleted in silicon compared to the higher-temperature deposits. Materials prone to calcium corrosion would be much more severely attacked by this type of deposit than by the first. In addition, Figure 2 shows that the deposit contains a high level of sulfur and that the sulfur condenses after ash deposition. The sulfur also can be quite corrosive, especially to alloys.

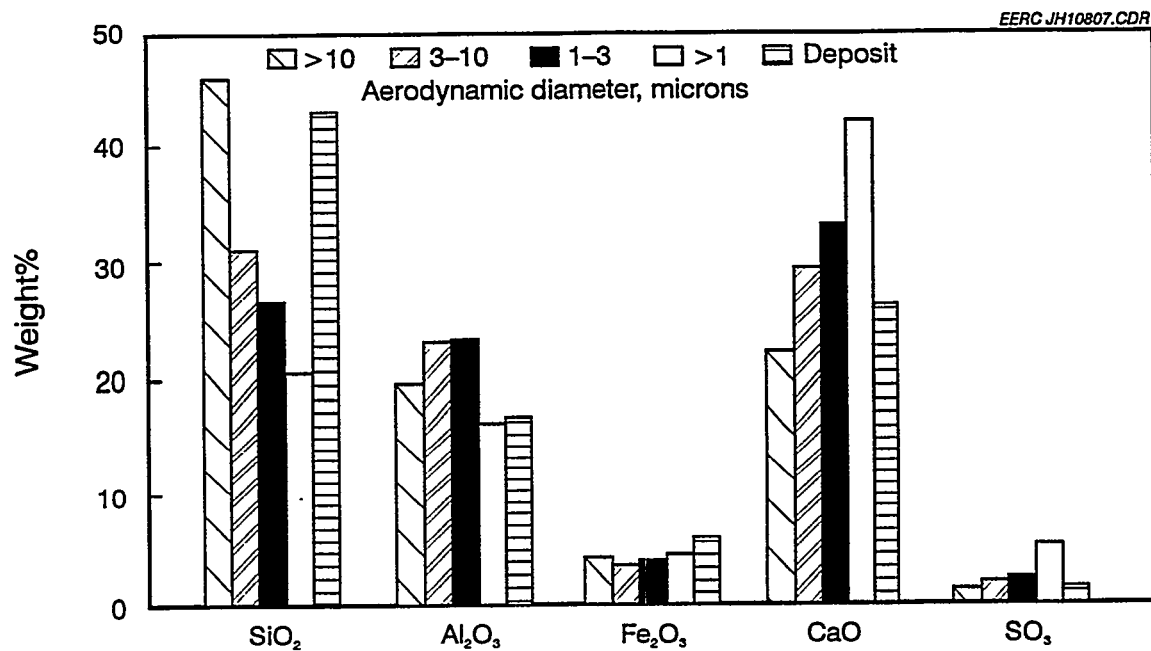


Figure 1. Comparison of the compositions (SO<sub>3</sub>-free) of the aerodynamically sized entrained ash particles and a conventional fouling deposit.

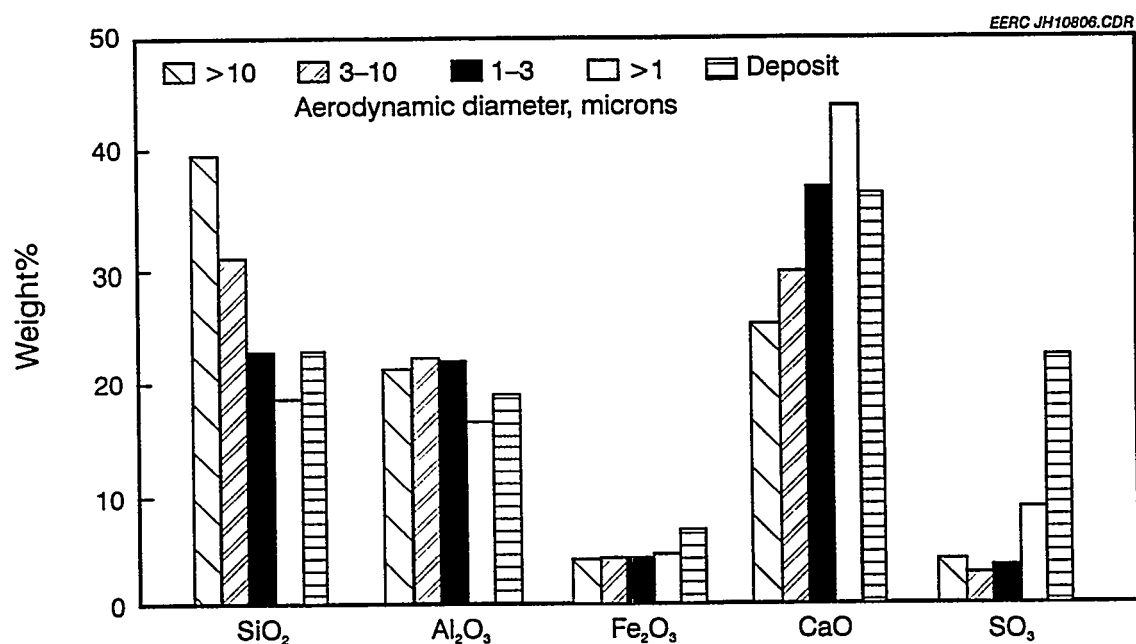


Figure 2. Comparison of the compositions (SO<sub>3</sub>-free) of the aerodynamically sized entrained ash particles and an upstream enamel deposit.

## 2.3 Factors Related to the Temperature of the Material

The temperature of the subsystem affects not only the kinetics of reaction but the composition and physical nature of the ash deposit as well. Figure 3 shows the concentrations of silicon, calcium, and sulfur in ash deposits collected from steam tubes in a boiler firing a high-calcium coal. It shows that the sulfur concentration in the deposits increases dramatically at temperatures below 2000°F. Laboratory experiments show that the mechanism of increase is chemical vapor deposition caused by the conversion of calcium in either oxides or aluminosilicates to calcium sulfate below 1900°F. Figure 4 shows the concentrations of sodium, potassium, and phosphorus in the same deposits. They also increase significantly, but not as much as that of the sulfur. The sodium concentration increases primarily through physical vapor deposition, or condensation, of sodium sulfate. This indicates that in the presence of ash, materials cooled to below approximately 1900°F will be subjected to alkali sulfate corrosion whereas those at higher temperatures will not. This may be especially prevalent for heat exchangers operating at gas temperatures above 1900°F but with surface temperatures below.

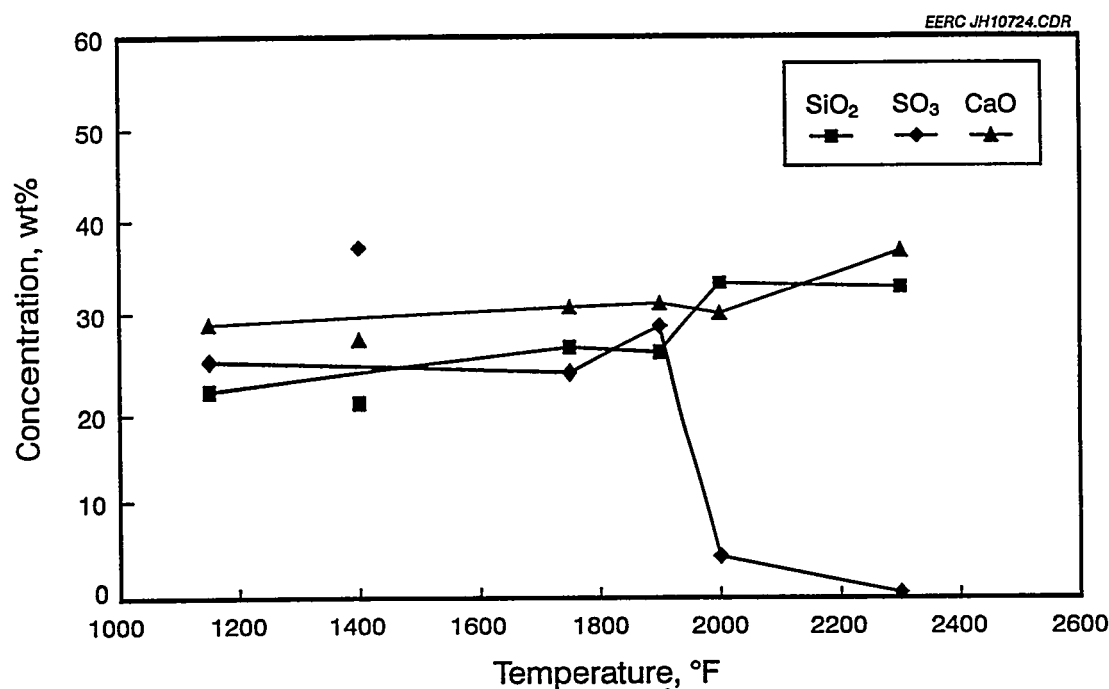


Figure 3. Temperature-dependent concentrations of silicon, sulfur, and calcium (reported as oxides) in deposits collected from the convective pass of a pulverized coal-fired utility boiler burning a subbituminous coal from the western United States.

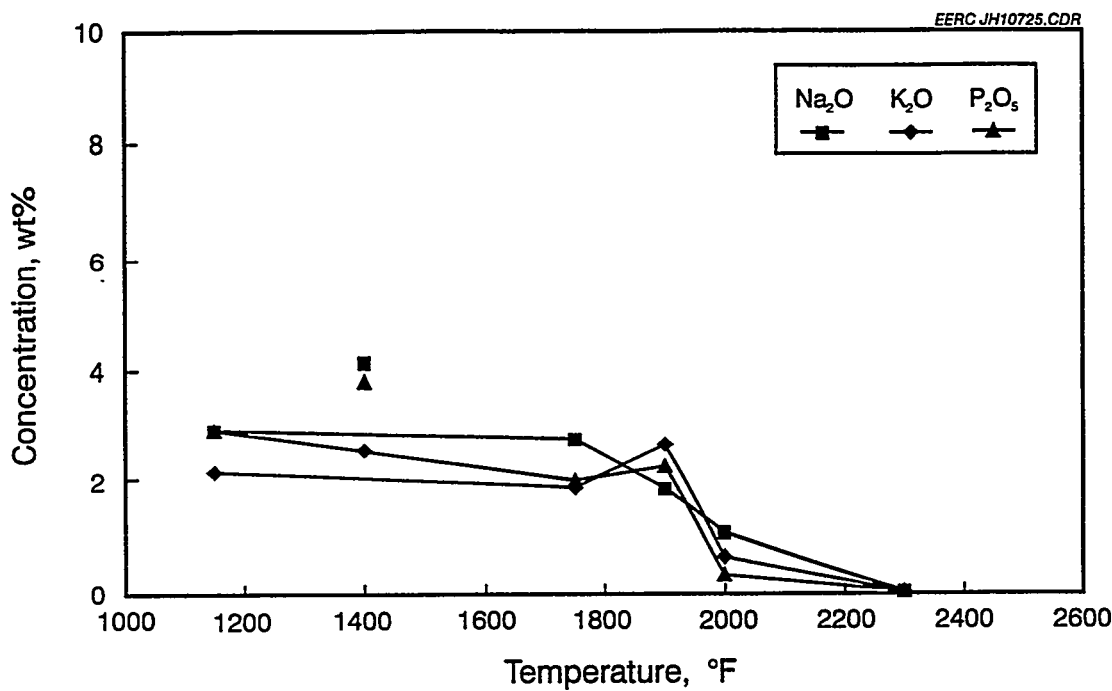


Figure 4. Temperature-dependent concentrations of sodium, potassium, and phosphorus (reported as oxides) in deposits collected from the convective pass of a pulverized coal-fired utility boiler burning a subbituminous coal from the western United States.

In addition to affecting composition, temperature will affect the physical nature of the deposits. Figure 5 shows a viscosity-versus-temperature plot for fused slag formed in a Central Illinois Public Service Coffeen Plant boiler while burning Illinois No. 6 bituminous coal to which limestone has been added to reduce the viscosity of the slag. The measurements were made in air and in a reducing environment in the presence of 10% water vapor. At temperatures above 2500°F, the slag has a viscosity below 250 poise implying that it will flow and so will be erosive as well as corrosive. These liquid slags dissolve the protective oxide scale on most ceramic materials, causing the corrosion rate to be linear rather than parabolic with time. Corrosion by flowing slag is expected to result in a uniform recession rate of the surface, while pitting is seen in corrosion by static slag or with sintered ash. Figure 6 is a scanning electron micrograph of a cross section of Hexoloy SA silicon carbide exposed to another Illinois No. 6 slag at 2300°F in a static corrosion test performed in air (4). The bright spheres are composed of iron silicide that form near pits in the silicon carbide. The pitting may weaken the material, although the recession rate is reduced as compared to flowing slag corrosion.

At still lower temperatures, the ash may sinter but does not dissolve the protective oxide layer. Figure 7 is a scanning electron micrograph of the interface between siliconized silicon carbide (bottom) and a fine high-calcium ash doped with excess sodium sulfate (top) and reacted in air at 1790°F. Scanning electron microscopy (SEM) analyses show that the scale is composed of calcium and magnesium silicate. Only very low levels of sodium could be measured in the scale,

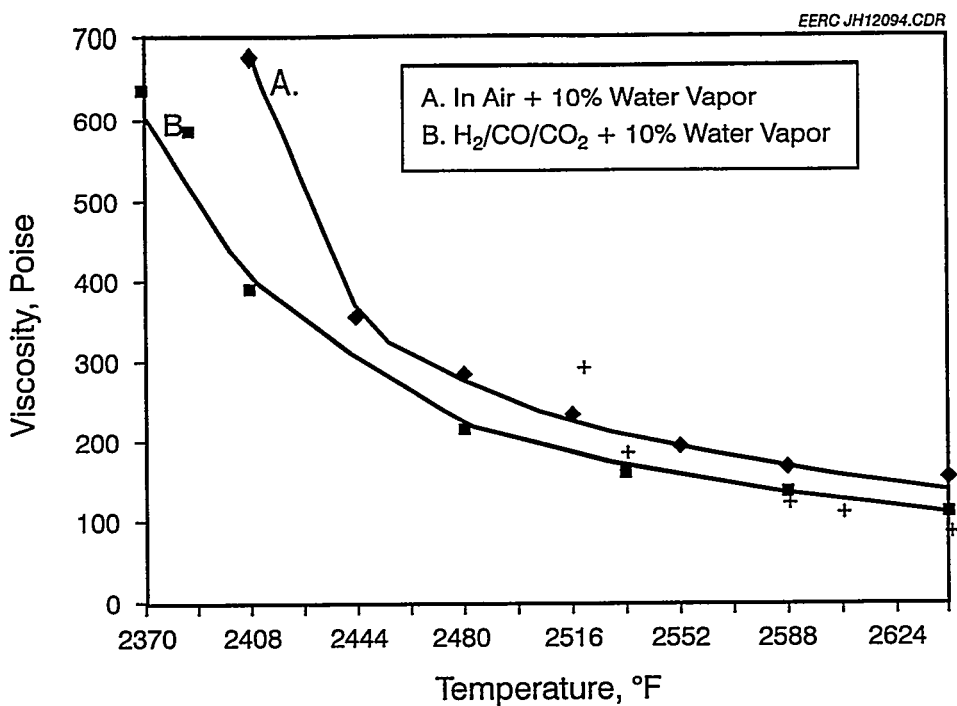


Figure 5. Viscosity-versus-temperature plot for a slag produced in a boiler firing Illinois No. 6 bituminous coal to which limestone has been added to reduce slag viscosity.

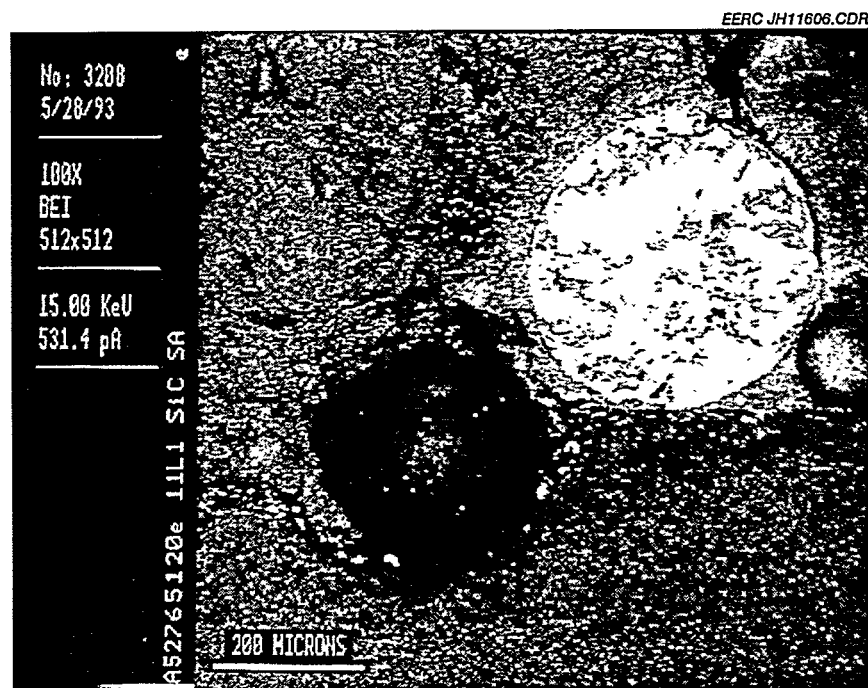


Figure 6. Scanning electron micrograph of a cross section of Hexoloy SA silicon carbide (bottom) exposed to Illinois No. 6 slag at (top) 2300°F in a static slag corrosion test in air.

but similar experiments performed without the condensed sodium sulfate show that the oxidation rate of the material is greatly increased by the presence of the sodium. Sodium silicate does not form extensively in this situation because it is not stable in the presence of aluminosilicate ash.

### 3.0 THE EFFECTS OF SPECIFIC ELEMENTS IN THE CORROSION OF SILICON-BASED CERAMICS

Approximately a dozen inorganic elements in the products of coal combustion affect the corrosion rates of silicon-based ceramics used to construct subsystems. The elements, including H, O, Na, Mg, Al, Si, P, S, Cl, K, Ca, and Fe, affect corrosion rates in three ways: as primary corrodents that form reaction products with the material, as secondary corrodents that affect the activity of the primary corrodents, or by influencing the rate of mass transfer of the primary corrodents. Although many of the elements function as more than one type of corrodent, they are listed here under what is believed to be their most active role.

The primary corrodents of silicon-based ceramics in coal-fired combustion systems include O, Mg, Ca, and Fe. These elements form silicates or silicides that are stable in the presence of the other constituents of the ash in contact with the ceramic surface. Examples of their corrosion products are shown in Figures 6 and 7. When ash is not present, such as downstream of a filter, vapor-phase sodium can also be a primary corrodent of silicate ceramics, forming a sodium-enriched reaction layer through which oxygen can more rapidly diffuse than through a pure silica layer (15).

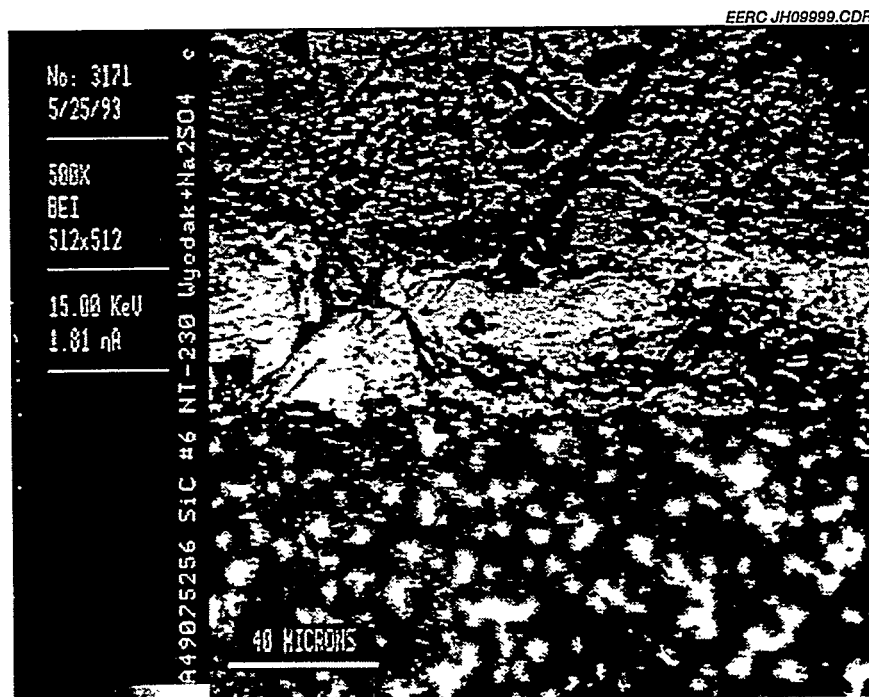


Figure 7. Scanning electron micrograph of the interface between siliconized silicon carbide (bottom) and a high-calcium ash doped with excess sodium sulfate (top) reacted at 1790°F.

In contrast to the primary corrodents, the secondary corrodents in coal combustion tests have not been observed to form corrosion products with silica- or alumina-based ceramics. They are known, however, to affect the activities of some of the primary corrodents. The main elements acting in this role are H, Al, S, and Cl. Hydrogen is most important in gasification conditions because it affects the concentration of O; in combustion conditions, it helps to form volatile hydroxides such as  $\text{Si}(\text{OH})_4$  or NaOH which will affect corrosion rates when no other ash is present. Similarly, S and Cl affect the vapor-phase concentrations of  $\text{Na}_2\text{SO}_4$  and  $\text{NaCl}$ , which will affect corrosion rates when ash is not present. In addition, Al affects the activity of Na, Mg, and Ca. Since these elements are more stable in an aluminosilicate phase than in a silicate corrosion product, they are less corrosive to silicate ceramics when aluminum is present in the ash.

Finally, the major role of several other elements is their effect on the rate of transport of the primary corrodents. These elements include Na, Si, P, and K. They are most important in their effect on the viscosity of a melt, as well as on the rate of ion diffusion in a glass. They have not been observed to form corrosion products except in minor roles.

Because the concentrations of many of these elements affect the activities of the primary corrodents, the surest experimental design to determine all of the interdependencies is the full factorial matrix, where the concentration of each element in the system is varied independently on the others. However, the number of tests in such a matrix would involve  $X^n$  tests, where X is the number of variations of each element and n is the number of different elements. For three variations (low, medium, and high concentrations) of each of 12 elements, the number of tests is 531,441 for a single temperature and pressure condition. The numbers can be partially reduced with the use of a fractional factorial test matrix, but the most cost-effective way to perform corrosion tests is to base them on realistic system conditions.

The best method to obtain appropriate test conditions is to expose the material in an operating coal-fueled system. This can be expensive since a 100-hour pilot-scale test may cost \$50,000. As the scale of the test is reduced, so are the costs, but the accuracy of the conditions may also be compromised. To improve the accuracy of laboratory-scale test conditions and allow similar tests performed in different labs to be more comparable, the EERC has been surveying the literature and holding discussions with interested researchers and industry representatives to develop appropriate baseline test conditions. The conditions were chosen to be harsh yet realistic (i.e., not accelerated) and should include all of the primary and secondary corrodents. Two ceramic subsystems were the focus of the research: hot-gas particulate filters and high-temperature heat exchangers under both combustion and gasification conditions. Although one set of parameters for each of these conditions has been suggested as a baseline, it is strongly recommended that any test matrix include parametric testing.

### 3.1 Combustion Conditions

System conditions in coal combustors are well understood in the oxidizing zones downstream of the coal flame. Above 1650°F, the condensed ash is the most corrosive to ceramics. To assure that all researchers have access to identical ashes for their tests, the EERC has assembled 55-gallon drums of coal ash and slag from four utility power plants. Gallon quantities of each ash will be supplied for testing at no charge to the researchers. The samples were gathered by utility plant

workers from areas of the power systems where they best simulate the chemical and physical state of the ash in contact with either hot-gas particulate filters or high-temperature heat exchangers.

For testing ceramic-ash interactions in hot-gas filter systems, ash was provided by the American Electric Power (AEP) Company Tidd Plant from the Westinghouse advanced particulate filter (APF). The ash was collected in February 1995 while firing a Pittsburgh No. 8 coal and using a dolomite sorbent. In lab testing, the surfaces of the test filters can be coated by fluidizing the ash in a closed container around the filter and pulling a vacuum on the outlet of the filter. The air flow through the filter should be maintained as the filter is placed in the test reactor to prevent the cake from falling off. The suggested baseline temperature for these tests is 1650°F. Of course, any test matrix should include a range of temperatures down to approximately 1400°F, but we suggest that all researchers should include 1650°F as one of the temperatures because it is the maximum at which second-generation pressurized fluidized-bed combustion (PFBC) systems are expected to operate and because potential purchasers of these systems need to know how the materials will perform at extreme yet realistic conditions. This ash can also be used to test heat-exchanger materials that will operate in a PFBC downstream of a particulate removal device at temperatures below the sulfation temperature of the ash (approximately 1900°F).

The composition of the gas stream should also include primary and secondary corrodents in similarly extreme yet possible (not accelerated) concentrations. Since most hot-gas particulate filters will operate in pressurized systems, appropriate partial pressures of the gases should be used when possible. The concentrations of the major gases will differ little from combustor to combustor, although partial pressures will vary with system pressure. These concentrations can be easily predicted, assuming complete coal combustion. Unfortunately, little information exists about the concentrations of trace species in actual pressurized combustors. Therefore, we suggest using a gas composition similar to that measured by Radian Corporation at the entrance to the Westinghouse APF at the Tidd PFBC in the Spring of 1994. The data are yet to be published in final form, but AEP and DOE Morgantown Energy Technology Center (METC) personnel have allowed us to use it for the purposes of designing these tests. An initial set of conditions was presented by Hurley (1). They were discussed at the 9th Annual Conference on Fossil Energy materials at Oak Ridge. In addition, researchers at 16 leading research and industrial institutions were contacted by e-mail or fax to solicit any disagreements with the proposed conditions. They are Argonne National Laboratory, CeraMem Corporation, DuPont Lanxide Composites Incorporated, Electric Power Research Institute, Industrial Filter and Pump, Lurgi-Lentjes-Babcock, Minnesota Mining and Manufacturing (3M), Morgantown Energy Technology Center, Oak Ridge National Laboratory, Pall Separations, Penn State University, Refractron Tech Corporation, Schumacher Umwelt, Southern Research Institute, Virginia Polytechnic, and Westinghouse. Slight disagreements with the original conditions were received from Industrial Filter and Pump, Lurgi-Lentjes-Babcock, Penn State, and Westinghouse. Most of their suggestions have been incorporated in the following final conditions. One exception is the temperature. Lurgi-Lentjes-Babcock suggested that it be dropped to 850°C, while Industrial Filter and Pump suggested higher temperatures, so we kept the originally proposed temperature for the baseline tests.

The primary gases that must be included are NaCl, SO<sub>2</sub>, HCl, O<sub>2</sub>, H<sub>2</sub>O, and N<sub>2</sub> since they either corrode silicon- and aluminum-based ceramics, or they affect the activity of the corrodents. For a one-atmosphere lab test, it is suggested that the gas composition be 10 ppmv NaCl, 3300

ppmv  $\text{SO}_2$ , 1100 ppmv  $\text{HCl}$ , and 300,000 ppmv (30%)  $\text{O}_2$ . The partial pressures for  $\text{NaCl}$ ,  $\text{SO}_2$ , and  $\text{HCl}$  are three times as high as those measured at Tidd (yet less than other values reported by Mann and others [16]) to assure that appropriate but harsh conditions are simulated. For  $\text{H}_2\text{O}$ , the proper partial pressure would be approximately 1.5 atmospheres which is not possible in a 1-atmosphere test, so it is suggested to use only 150,000 ppmv (15%) which is relatively easily reached experimentally. The balance should be nitrogen. Carbon dioxide is not necessary since at these temperatures in the presence of  $\text{SO}_2$ , sulfates are more stable than carbonates. It is suggested to use dry air as the feed and simply enriching it with additional  $\text{O}_2$  and the other gases to reach the concentrations listed here.

To simulate the type of ash that will strike a high-temperature heat exchanger upstream of ash removal devices, slags were gathered from the taps of three cyclone-fired boilers. Subbituminous coal slag was provided by the Northern States Power Company Riverside Plant, which was burning a coal from the Powder River Basin in Wyoming. Illinois No. 6 bituminous coal slag was provided by the Central Illinois Public Service Coffeen Plant. Analyses showed abnormally high calcium concentrations in this slag owing to limestone additions to the coal to reduce slag viscosity. Therefore, another drum of more "pure" Illinois No. 6 slag was obtained from the Illinois Power Company Baldwin Plant. Suggested initial conditions for slag testing are 2000°F for sintered ash conditions, 2300°F for viscous molten ash, and 2600°F for runny molten ash. All of the EERC tests were run in air, although some measurements show that water vapor may significantly affect slag viscosity and perhaps should be included at a level of about 15%. This is still being investigated. The slag layer thickness should be approximately 1 millimeter at 2600°F and 5 millimeters at 2300°F to ensure appropriate oxygen transport. It should be replenished often enough that it does not become overly concentrated with corrosion products. The compositions of the ashes are shown in Table 2. The viscosity-versus-temperature curves under both oxidizing and reducing conditions of the Coffeen slag are shown in Figure 5, whereas the curves for the other two slags are shown in Figure 8.

### 3.2 Gasification Conditions

Gasification conditions are much more difficult to simulate in the laboratory because of the wide range of gas temperatures and compositions possible in the different systems. During gasification, coal is heated in the presence of insufficient oxygen to completely burn. Carbon monoxide and hydrogen are among the major product gases. Variations in system pressure and temperature strongly affect the concentrations of the gases in the product. Also, to keep the calorific value of the gas as high as possible, some gasifiers operate with pure oxygen rather than air so that the gas is not diluted with inert nitrogen. This is especially true in the first integrated gasification combined cycle (IGCC) systems because at the time of their design, low-Btu gas burners were not reliable. However, advances in burner design over the last decade will permit air-blown product gas to be burned efficiently in future IGCC systems. These will include the Sierra Pacific Pinon Pine Power Project and the Foster Wheeler carbonizer to be used in the Four Rivers Energy Modernization Project and in the Combustion 2000 High-Performance Power System (HiPPS).

There are three main types of coal gasifiers currently in use: entrained-flow systems such as the pressurized Shell, Texaco, and Dow gasifiers and the atmospheric Koppers-Totzek gasifier; fluidized-bed systems such as the Winkler or Kellogg-Rust-Westinghouse (KRW) gasifiers; and a

TABLE 2

## Chemical Compositions of Standard Ashes

| Oxide, wt%                     | Tidd Ash | Riverside Slag | Coffeen Slag | Baldwin Slag |
|--------------------------------|----------|----------------|--------------|--------------|
| SiO <sub>2</sub>               | 24.1     | 47.0           | 52.5         | 53.4         |
| Al <sub>2</sub> O <sub>3</sub> | 7.7      | 18.6           | 16.3         | 18.6         |
| Fe <sub>2</sub> O <sub>3</sub> | 6.4      | 5.3            | 13.5         | 17.6         |
| TiO <sub>2</sub>               | 0.3      | 1.4            | 0.7          | 0.7          |
| P <sub>2</sub> O <sub>5</sub>  | 0.2      | 0.6            | 0.2          | 0            |
| CaO                            | 28.8     | 19.7           | 13.1         | 7.1          |
| MgO                            | 16.2     | 5.7            | 1.2          | 0.9          |
| Na <sub>2</sub> O              | 0.2      | 0.9            | 0.8          | 0.0          |
| K <sub>2</sub> O               | 0.8      | 0.3            | 1.6          | 1.7          |
| SO <sub>3</sub>                | 15.2     | 0.3            | 0.1          | 0.0          |

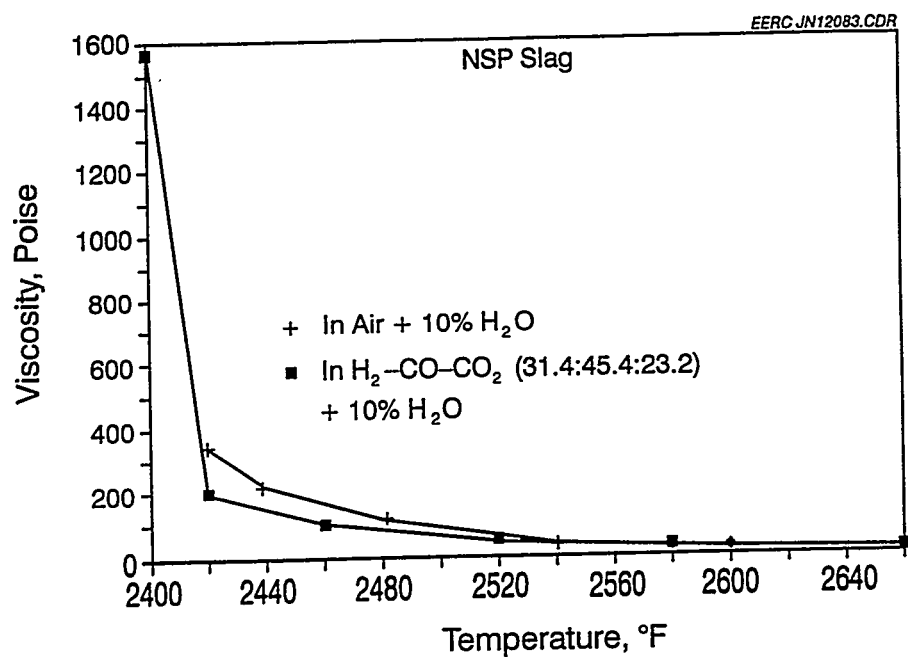
fixed-bed system used by Lurgi. The range of measured operating temperatures and product gas compositions for these three types of gasifiers as reported by Watkinson and others (17) are listed in Table 3. The coals used range in rank from lignite to bituminous, and all systems shown were oxygen-blown.

Because of the wide range of gasifier designs and operating conditions, it is difficult to choose one set of conditions for baseline testing of ceramic materials. As in combustion, two main subsystems should be addressed, hot-gas particle filters and heat exchangers. In most of the new oxygen-blown gasifier systems such as the Tampa Electric (Texaco), Wabash River (Dow), and Buggenum, Netherlands (Shell), projects, particulate cleanup will be performed in relatively cool gas of around 500°F so ceramic corrosion should not be a problem. The Tampa project will include some hot-gas particulate cleanup at 1000°F, but they are proposing to use metal filters. Therefore, our recommendation is to run ceramic particle filter gasification corrosion studies in conditions that will be experienced in the Sierra Pacific Power Company Pinon Pine Power Project fluidized-bed gasifier. The gasifier is an air-blown 102-MWe unit employing a Westinghouse ceramic particle filter system operating at as high as 1100°F at 300 psia. Expected gas compositions in the filter will be approximately 25% CO, 15% H<sub>2</sub>, 5% CO<sub>2</sub>, 5% H<sub>2</sub>O, and 50% N<sub>2</sub>. Vapor-phase sodium chloride concentrations are expected to be ten to one hundred times the levels in combustion systems, but in general the concentrations of the minor primary and secondary corrodents have not been measured nor are they well defined.

#### 4.0 SUMMARY

For a given temperature, the rate of corrosion of ceramic materials in advanced coal-fired energy systems is affected by the composition of the gas and condensed species in contact with the material. These compositions are dependent on the fuel (and sorbent in a fluidized-bed system), which determines what species will be present; the temperature of the material, which determines

(a)



(b)

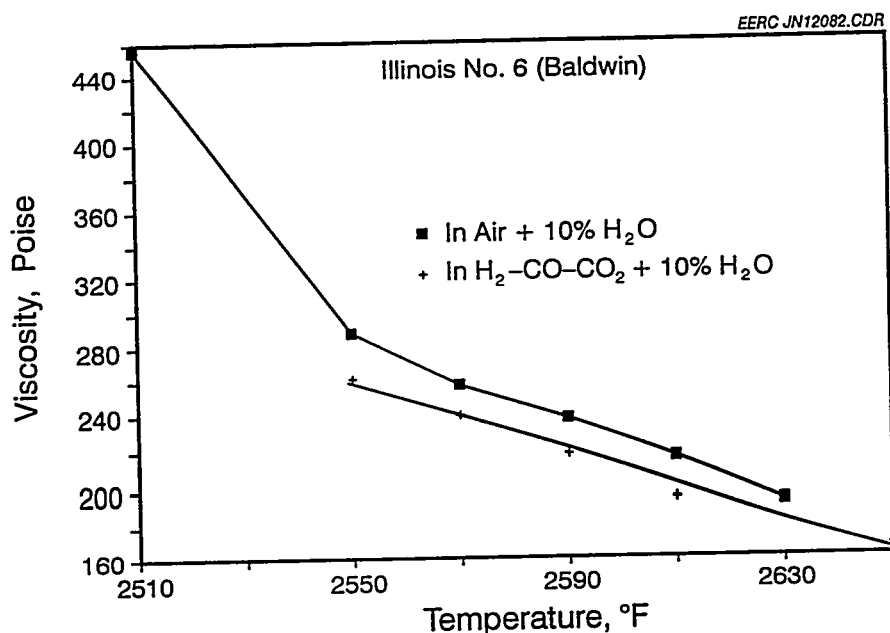


Figure 8. Viscosity-versus-temperature curves in air and reducing conditions for the three slags listed in Table 2: (a) Riverside Powder River Basin slag (b) Baldwin Illinois No. 6 slag.

TABLE 3

## Typical Operating Conditions for the Main Types of Oxygen-Blown Gasifiers

|                  | Entrained Flow<br>Average | Range   | Fluidized Bed<br>Average | Range   | Fixed Bed (Slagger)<br>Average | Range   | Fixed Bed (Dry Ash)<br>Average | Range   |
|------------------|---------------------------|---------|--------------------------|---------|--------------------------------|---------|--------------------------------|---------|
| Temperature, °F  | 2150-2500                 |         | 1700-1890                |         | 2280-2880                      |         | 1440-1510                      |         |
| Pressure, psia   | 15-610                    |         | 15-370                   |         | 310-360                        |         | 390-450                        |         |
| Gas Composition  |                           |         |                          |         |                                |         |                                |         |
| CO               | 54                        | 41-62   | 37                       | 26-51   | 57                             | 56-58   | 17                             | 16-18   |
| H <sub>2</sub>   | 32                        | 30-35   | 39                       | 32-45   | 28                             | 27-28   | 39                             | 39-40   |
| CO <sub>2</sub>  | 6.4                       | 2-10    | 19                       | 10-39   | 3.8                            | 3.3-4.3 | 31                             | 30-32   |
| CH <sub>4</sub>  | 0.1                       | 0-0.3   | 3.0                      | 1.8-5.0 | 6.6                            | 6.5-6.7 | 10                             | 9-11    |
| N <sub>2</sub>   | 1.9                       | 0.8-4.7 | 0.7                      | 0.5-0.9 | 2.4                            | 0.6-4.3 | 1.2                            | 0.8-1.5 |
| H <sub>2</sub> S | 1.1                       | 0.3-1.8 | 1.4 <sup>a</sup>         |         | 1.3                            | 0.6-2.0 | 1.4 <sup>a</sup>               |         |
| COS              | 0.1 <sup>a</sup>          |         | 0.0 <sup>b</sup>         |         | 0.0 <sup>b</sup>               |         | 0.0 <sup>b</sup>               |         |
| H <sub>2</sub> O | 4.4 <sup>c</sup>          |         | 0.0 <sup>b</sup>         |         | 0.0 <sup>b</sup>               |         | 0.0 <sup>b</sup>               |         |
| No. of Systems   | 4                         |         | 5                        |         | 2                              |         | 2                              |         |

<sup>a</sup> 1 in estimate.<sup>b</sup> No data, values estimated.<sup>c</sup> By difference because of lack of data.

whether vaporized species will have condensed and whether the ash is molten; and the local gas flow conditions, which determine the size range of ash depositing and therefore the composition of the ash. Approximately 12 elements affect the corrosion rates of silicon- and aluminum-based ceramics under combustion conditions. O, Mg, Ca, Fe, and Na when no ash is present are primary corrodents in that they have been observed to form corrosion products with silicon carbides. Secondary corrodents—H, Al, S, and Cl—have not been observed to form primary corrosion products under coal combustion conditions but do affect the activity of the primary corrodents. The other major elements, including Na, Si, P, and K, affect the rate of transport of the primary corrodents by affecting slag viscosity and ion mobility. In general, very little work has been done under reducing conditions so the primary and secondary corrodents in gasifier systems are not well understood at this time.

To improve the accuracy of laboratory-scale combustion test conditions and assure comparability between testing groups, the EERC has assembled 55-gallon drums of coal ash and slag from four utility power plants, portions of which will be provided free of charge to investigators. The samples were gathered by utility plant workers from areas of the power systems where they best simulate the state of the ash in contact with either hot-gas particle filters or high-temperature heat exchangers.

For hot-gas filter testing, ash from the AEP Tidd hot-gas filter is available. Although parametric tests are encouraged, a baseline test is proposed at 1650°F to simulate a harsh but realistic condition. For a one-atmosphere lab test, it is suggested that the gas composition should be 10 ppmv NaCl, 3300 ppmv SO<sub>2</sub>, 1100 ppmv HCl, and 300,000 ppmv (30%) O<sub>2</sub>, 150,000 ppmv (15%) H<sub>2</sub>O, and a balance of nitrogen.

To simulate the type of ash that will strike a high-temperature heat exchanger in a combustion system upstream of ash removal devices, slags are available from three cyclone-fired boilers. Suggested initial conditions for slag testing are 2000°F for sintered ash conditions, 2300°F for viscous molten ash, and 2600°F for runny molten ash. We have run all of our tests in air, although viscosity tests show that water vapor may significantly affect slag viscosity and perhaps should be included at a level of about 15%. To assure appropriate oxygen transport the slag layer thickness in a static test should be approximately 1 millimeter for runny slag and 5 millimeters for viscous slags. The slag should be changed often enough to prevent it from becoming overly concentrated in corrosion products, since in a commercial system the slag will be constantly replenished.

Designing appropriate tests for gasification conditions is much more difficult because of the wide variety of operating conditions and the general lack of available data on the necessary corrodents to include in the tests. We believe that these conditions should be much better defined through conversations with materials researchers and system manufacturers. In addition, thermochemical modeling of both corrosion reactions and system conditions should be performed. Finally, samples of ash and slag produced in gasification systems should be obtained for use in corrosion testing.

## 5.0 REFERENCES

- 1 Hurley, J.P. "Factors Affecting the Corrosion Rates of Ceramics in Coal Combustion Systems" *In Proceedings of the 9th Annual Conference on Fossil Energy Materials*; Oak Ridge, 1995.
2. Ferber, M.K.; Tennery, V.J. "Behavior of Tubular Ceramic Heat Exchanger Materials in Acidic Coal Ash from Coal-Oil Mixture Combustion," *Ceram. Bull.* **1983**, 62 (2), 236-243.
3. Ferber, M.K.; Tennery, V.J. "Behavior of Tubular Ceramic Heat Exchanger Materials in Basic Coal Ash from Coal-Oil Mixture Combustion," *Ceram. Bull.* **1984**, 63 (7), 898-904.
4. Strobel, T.M.; Hurley, J.P.; Senior, C.L.; Holowczak, J.E. "Coal Slag Corrosion of Silicon Carbide-Based Ceramics in a Combustion Environment," *In Proceedings of the Symposium on Silicon Carbide-Based Structural Ceramics*; American Ceramic Society PAC RIM Meeting, Honolulu, HI, Nov. 7-10, 1993; pp 327-334.
5. Strobel, T.M.; Hurley, J.P.; Breder, K.; Holowczak, J.E. "Coal Slag Corrosion and Strength Degradation of Silicon Carbide-Alumina Composites," *Ceramics Engineering & Science Proceedings* **1994**, 15 (4), 579-586.
6. Senior, C.L.; Moniz, G.A.; Hurley, J.P.; Strobel, T.M. "Corrosion of Silicon Carbides by Ash and Vapor in a Coal Combustion Environment," *In Proceedings of the Symposium on Silicon Carbide-Based Structural Ceramics*; American Ceramic Society PAC RIM Meeting, Honolulu, HI, Nov. 7-10, 1993; pp 335-342.
7. Combustion Engineering Inc. *Combustion*, 3rd ed.; Rand McNally: Chicago, 1981; pp 35-57.
8. Hurley, J.P.; Schobert, H.H. "Ash Formation During Pulverized Subbituminous Coal Combustion, 1. Characterization of Coals and Inorganic Transformations During Early Stages of Burnout," *Energy & Fuels* **1992**, 6 (1), 47-58.
9. Hurley, J.P.; Schobert, H.H. "Ash Formation During Pulverized Subbituminous Coal Combustion, 2. Inorganic Transformations During Middle and Late Stages of Burnout," *Energy & Fuels* **1993**, 7, 542-553.
10. Walsh, P.M.; Sayre, A.N.; Loehden, D.O.; Monroe, L.S.; Beér, J.M.; Sarofim, A.F. *Prog. Energy Combust. Sci.* **1990**, 16, 327-346.
11. Benson, S.A.; Jones, M.L.; Harb, J.H. "Ash Formation and Deposition," In *Fundamentals of Coal Combustion for Clean and Efficient Use*; Smoot D., Ed.; Elsevier: Amsterdam, 1993; 299.
12. Baxter, L.L.; DeSollar, R.W. *Fuel* **1993**, 72, 1411.

13. Wibberley, L.J.; Wall, T.F. *Fuel* 1982, 61, 93-99.
14. Hurley, J.P.; Benson, S.A.; Erickson, T.A.; Allan, S.E.; Bieber, J. *Project Calcium Final Report*, DOE/MC/10637-3292, 1995.
15. Zheng, Z., Tressler, R.E.; Spear, K.E. "A Comparison of the Oxidation of Sodium Implanted CVD  $\text{Si}_3\text{N}_4$  With the Oxidation of Sodium-Implanted SiC Crystals," *Corrosion Science* 1992, 33 (4), 569-580.
16. Mann, M.D.; Swanson, M.L.; Yagla, S.L. "Characterization of Alkali and Sulfur Sorbents for Pressurized Fluidized-Bed Combustion" *In Proceedings of the 13th International Fluid Bed Conference*; ASME; 1995.
17. Watkinson, A.P.; Lucas, J.P., Lim C.J. "A Prediction of Performance of Commercial Coal Gasifiers" *Fuel* 1991, 70, 519-527.

## DISTRIBUTION LIST

3M COMPANY  
M.A. Leitheiser  
R. Smith

AIR PRODUCTS AND CHEMICALS  
S.W. Dean

ALLISON GAS TURBINE DIVISION  
P. Khandelwal  
R.A. Wenglarz

AMA RESEARCH & DEVELOPMENT  
CENTER  
T.B. Cox

ARGONNE NATIONAL LABORATORY  
W.A. Ellingson  
J.P. Singh

ARGONNE NATIONAL  
LABORATORY-WEST  
S.P. Henslee

ARMY MATERIALS TECHNOLOGY  
LABORATORY  
SLCMT-MCC  
D. R. Messier

AVCO RESEARCH LABORATORY  
R. J. Pollina

BABCOCK & WILCOX  
T. I. Johnson

BABCOCK & WILCOX  
DOMESTIC FOSSIL OPERATIONS  
M. Gold

BRITISH COAL CORPORATION  
J. Oakey

CANADA CENTER FOR MINERAL &  
ENERGY TECHNOLOGY  
R. Winston Revic  
Mahi Sahoo

CERAMEM CORPORATION  
B. Bishop

DOE OAK RIDGE OPERATIONS  
Assistant Manager for Energy  
Research & Development

DOE OAK RIDGE OPERATIONS  
E.E. Hoffman  
M.H. Rawlins

DOE  
OFFICE OF BASIC ENERGY SCIENCES  
J.B. Darby

DOE  
IDAHO OPERATIONS OFFICE  
R.B. Loop

DOE  
MORGANTOWN ENERGY TECHNOLOGY  
CENTER  
R.C. Bedick  
D.C. Cicero  
F.W. Crouse, Jr.  
R. Dennis  
N.T. Holcombe  
W.J. Huber  
T. McMahon  
J.E. Notestein

DOE  
OFFICE OF FOSSIL ENERGY  
J.P. Carr

DOE  
OFFICE OF VEHICLE AND ENERGY  
R&D  
R.B. Schulz

DOE  
OFFICE OF SCIENTIFIC AND  
TECHNICAL INFORMATION

DOE  
PITTSBURGH ENERGY TECHNOLOGY  
CENTER  
A.L. Baldwin  
G.V. McGurl  
R. Santore  
T.M. Torkos

DOW CORNING CORPORATION  
H. Atwell

DUPONT COMPOSITES INC.  
D. Landini

EC TECHNOLOGIES  
D. J. Kenton

ELECTRIC POWER RESEARCH  
INSTITUTE  
R. Brown  
W.T. Bakker  
J. Stringer

ENERGY & ENVIRONMENTAL  
RESEARCH CENTER  
S. Benson  
B. Dockter  
T. Strobel

EUROPEAN COMMUNITIES JOINT  
RESEARCH CENTRE  
M. Van de Voorde

GA TECHNOLOGIES, INC.  
T.D. Gulden

GEORGIA INSTITUTE OF TECHNOLOGY  
T.L. Starr

IDAHO NATIONAL ENGINEERING  
LABORATORY  
B. H. Rabin

INDUSTRIAL FILTER AND PUMP  
P. Eggerstedt

LAVA CRUCIBLE-REFRACTORIES  
COMPANY  
T. Mulholland

LAWRENCE LIVERMORE NATIONAL  
LABORATORY  
W.A. Steele

LOS ALAMOS NATIONAL LABORATORY  
J.D. Katz

LURGI LENTJES BABCOCK  
G. von Wedel

NATIONAL INSTITUTE OF STANDARDS  
AND TECHNOLOGY  
S.G. Malghan

NATIONAL MATERIALS ADVISORY  
BOARD  
K.M. Zwilsky

OAK RIDGE NATIONAL LABORATORY  
P.T. Carlson  
N.C. Cole  
R.R. Judkins  
L. Kupp  
R.A. Lawson (8 copies)  
D. P. Stinton  
P. Tortorelli

OFFICE OF NAVAL RESEARCH  
S. G. Fishman

SANDIA NATIONAL LABORATORIES  
R.J. Buss  
G.A. Carlson  
A.G. Sault

SHELL DEVELOPMENT COMPANY  
L.W.R. Dicks

TENNESSEE VALLEY AUTHORITY  
C.M. Huang

THE JOHNS HOPKINS UNIVERSITY  
R.E. Green, Jr.

THE MATERIALS PROPERTIES  
COUNCIL, INC.  
M. Prager

THE NORTON COMPANY  
N. Corbin

PALL SEPARATIONS  
J. Sawyer

PENN STATE UNIVERSITY  
K. Spear  
R. Tressler

REFRACTON TECHNOLOGY  
CORPORATION  
C. Scheckler

SCHUMACHER UMWELT  
M. Durst

SOUTHERN RESEARCH INSTITUTE  
D. Pontius

THE TORRINGTON COMPANY  
W.J. Chmura

UNION CARBIDE CORPORATION  
H. Cheung

UNITED TECHNOLOGIES RESEARCH  
CENTER  
K.M. Prewo

UNIVERSITY OF WASHINGTON  
T.G. Stoebe

VIRGINIA POLYTECHNIC INSTITUTE &  
STATE UNIVERSITY  
J. Brown  
W.A. Curtin  
K.L. Reifsnider

WESTERN RESEARCH INSTITUTE  
V.K. Sethi

WESTINGHOUSE ELECTRIC  
CORPORATION  
S.C. Singhal